https://doi.org/10.20965/jrm.2013.p0506

Paper:

Development of Method Using a Combination of DGPS and Scan Matching for the Making of Occupancy Grid Maps for Localization

Junji Eguchi and Koichi Ozaki

Utsunomiya University
7-1-2 Yoto, Utsunomiya-city, Tochigi 321-8585, Japan
E-mail: eguchi@ir.ics.utsunomiya-u.ac.jp
[Received October 19, 2012; accepted April 20, 2013]

This paper describes a method of making an occupancy grid map through the combined use of DGPS and scan matching. In outdoor environments such as city areas, high-accuracy localization is required for autonomous navigation. Scan matching with a laser scanner and an occupancy grid map consisting of precise structure information on the environment is one of the most accurate localization methods. However, mismatching on the map sometimes occurs, resulting in the robot losing its own position. Although a GPS device, an absolute positioning device, is valid for estimating position and attitude to a certain degree of accuracy, GPS often obtains erroneous positions for multipath problems which occur around tall buildings. In order to estimate the position and attitude of robots more stably, the authors have developed a method of making an occupancy grid map, which corresponds to DGPS directions and has an accurate shape, by using of some accurate DGPS measurement points and the SLAM method. In autonomous navigation, the robot trajectory is estimated using the particle filter method, evaluation and resampling are done using the two ways mentioned above, and attitude is calculated using DGPS measurement points and the result of scan matching. In this paper, the performance of the map-making method and localization method for autonomous navigation is shown through experiments which are evaluated as to the accuracy of the map in an actual environment.

Keywords: autonomous mobile robot, SLAM, GPS, laser scanner, particle filter

1. Introduction

Recent research and development has been focused on outdoor autonomous mobile robots for use in ordinary living environments in which people come and go. The authors of this paper participated in the "Tsukuba Challenge" project [1], open experiments held in Tsukuba, Ibaraki Prefecture, Japan from 2007 through 2011 to demonstrate the abilities of autonomous mobile robots in ordinary living environments. The task course set up in the "Tsukuba Challenge 2011," about 1.4 km in length, involved sidewalks, walking paths through parks, Tsukuba Center in the city center where many people come and go, elevators that people get on and off, etc. In order to achieve stable autonomous navigation in such diverse environments, high-accuracy localizations in those environments was crucially important.

Relatively high-accuracy methods of localization in outdoor environments include scan matching with occupancy grid maps prepared previously [2–4]. Laser scanners using laser beams to scan are often used in the scan matching to sense objects and shapes in the environments. Localizations as accurate as several centimeter can be realized by searching the positions and attitudes of scan data as a result of the observation of environments corresponding with the occupancy grid maps; this is hereinafter called matching.

In environments with fixed objects such as buildings or trees (hereinafter called landmarks) which will enable stable matching with occupancy grid maps, a robot can navigate autonomously using its own localizations. In environments with fewer landmarks, however, mismatching between landmarks and unknown objects such as pedestrians could occur, leading to localization failures [5].

On the other hand, there is another method of obtaining absolute positional data in outdoor environments: DGPS. It can provide positioning as accurate as 50 cm with radio wave signals from artificial satellites. DGPS, which is GPS with some additional correction data provided, should be a more accurate positioning system than GPS. Using DGPS, almost constantly accurate localizations are possible in the environments in which radio waves from artificial satellites can be directly received.

Scan matching and DGPS positioning should be applied in different environments. In other words, the combined use of scan matching and DGPS positioning could each make up for the other's shortcomings.

In this study, we have developed an occupancy grid mapping method to realize localizations through the combined use of scan matching and DGPS positioning. We have also carried out navigation experiments involving an autonomous mobile robot in outdoor environments to verify the effectiveness of localizations provided by the combined use of DGPS positioning and scan matching.

2. Related Studies and Approach of This Study

Localizations by means of DGPS are made using positioning points with accuracies which stays within a range of preset errors. However, errors in actual DGPS positioning depend on the environments to a great extent. In environments with tall buildings in particular, positioning accuracy tends to decrease due to the effects of multipath caused by the diffraction and reflection of radio wave signals. Using DGPS positioning for autonomous navigation, therefore, would require constant evaluations of the positioning accuracies [6, 7]. Takeuchi et al. proposed a method of using three-dimensional maps which include buildings around the task course [8]. Any positioning values that may include signals from invisible artificial satellites are rejected by determining the visibility of GPS satellites from the robot's current position. That method could prevent any decrease in positioning accuracy due to multipath caused by the reflection of radio wave signals from artificial satellites, it could also achieve relatively high positioning accuracy. Kitamura et al. proposed a method of directly determining the visibility of GPS satellites [9]. Their method can distinguish obstacle areas and empty areas in the whole sky images, as signals from artificial satellites in the obstacle areas are rejected, positioning accuracy with GPS can be maintained. Those methods, however, need to sense surrounding environments and would require large and complicated systems.

On the other hand, scan matching requires occupancy grid maps to be prepared beforehand. Hara et al. created occupancy grid maps with relatively high conformity in directions and shapes with the framework of a particle filter, using robot's navigation models, scan data from laser scanners, and the intensity of received light [10]. That method would probably work for relatively short distances in indoor environments surrounded by landmarks. Applied in outdoor environments with fewer landmarks and long distances, the method would have enormous calculation costs, and the success rates of mapping would decrease. In Date et al.'s method for outdoor mapping, the arrangement of scan data was adjusted so that any errors in overlapped scan data and any differences from GPS coordinates would be kept at the minimum [11]. The overlapping of scan data is effective in resolving any deviations in the landmark coordinates as observed at each time the robot carries out autonomous navigation in the overlapped areas of a task course through which it passes more than once. In other areas of the task course, no large errors in directions or shapes on the maps would occur if GPS positioning points were used for reference.

In contrast to the abovementioned methods, our approach to the occupancy grid mapping is to switch the two methods of DGPS positioning and scan matching. In unknown areas through which the robot passes for the first time, we estimate its trajectories using highly accurate DGPS points, while in known areas where the robot has passed more than once, we estimate the trajectories using scan matching. On the maps made this way, directions will correspond with those gotten using DGPS positioning, and there will occur no unconformity with respect to landmarks. To achieve stable autonomous navigation, errors in relative localizations in the environments should be as small as possible. In this study, therefore, we have defined accuracies in localizations by the variability in the pathways along which the robot repeatedly navigates or by the reproducibility of the trajectories.

Fig. 1. Course environment.

3. Occupancy Grid Mapping Method Based on DGPS Positioning

3.1. Setting of Task Course

We set up a course approximately 860 m long around the campus of the Engineering Faculty of Utsunomiya University (Japan), shown in **Fig. 1**, to provide for the occupancy grid mapping. The robot was to take the following pathways in the order marked in **Fig. 1**: R1-R2-R3-R4-R1-R5-R6-R7-R1. In this course, any deviations in the trajectories on the overlapped pathway R1 caused by the errors in localizations need to be coordinated: an issue of trajectory matching (hereinafter called loop closing). In the sections surrounded by buildings, DGPS positioning accuracies tend to decrease due to multipath. Furthermore, gyro errors become larger in the curved sections or corners where the navigation directions change widely. These errors in turn cause some errors in the gyro-odometry and require some correction of the trajectories. In other words, the conditions of the task course were ideal for the evaluation of the mapping method we developed. **Fig. 2** illustrates the structure of the developed occupancy grid mapping method. Black areas indicate landmarks observed by the laser scanner. White areas indicate the areas where the laser beam of the laser scanner has passed as the robot moves, which are defined as known areas. Gray areas represent unknown areas which have not been observed by the laser scanner. A group of green points in the particle filter indicate the particles. A

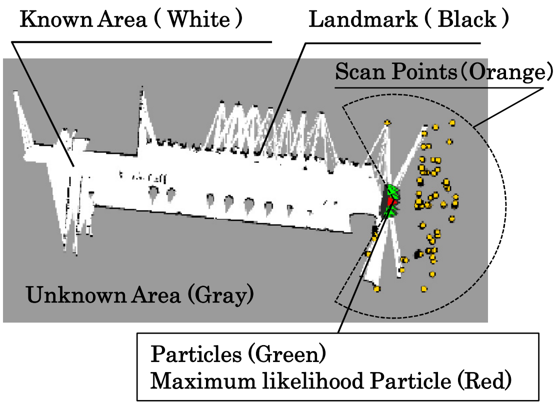

Fig. 2. Example of occupancy grid map.

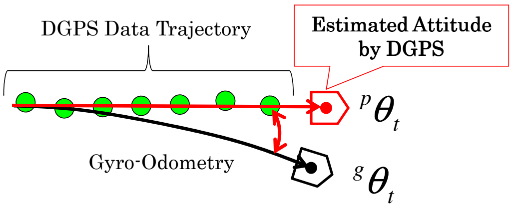

Fig. 3. Attitude estimation by means of principal component analysis.

red point indicates the maximum likelihood particle. Orange points indicate scan points emitted by the maximum likelihood particle.

3.2. Evaluation of DGPS Positioning Accuracies Using Approximate Lines

We aim to realize a much simpler and more versatile system for the evaluation of DGPS positioning accuracies without the use of other devices. Morales et al. proposed NIStest to distinguish outliers due to multipath in predicting the GPS positioning positions through localizations with the framework of Extended Kalman Filter methods (EKF) [12]. Their method makes use of the gyro-odometry and EKF to distinguish outliers due to multipath, so their positioning accuracies depend on the number of errors of the gyro-odometry. On the other hand, our proposed method uses DGPS positioning only, so that its accuracies do not depend on the gyro-odometry. When the robot navigates along a straight path, trajectories of DGPS positioning points can be approximated to straight lines, as illustrated in **Fig. 3**. We can then obtain inclination angles ${}^{p}\theta_t$ at any given time t through the principal component analysis of the trajectories of DGPS positioning points. The greater the contribution rates of the first principal component are, the more linear the trajectories of DGPS positioning points become. On the other hand, in the curved sections of the course, the greater the curvature is, the smaller the contribution rates of the first principal components become. At the forks in the course, where the direction changes in navigation are great, straight-line approximation accuracies decrease, and the contribution rates of the first principal component also decrease

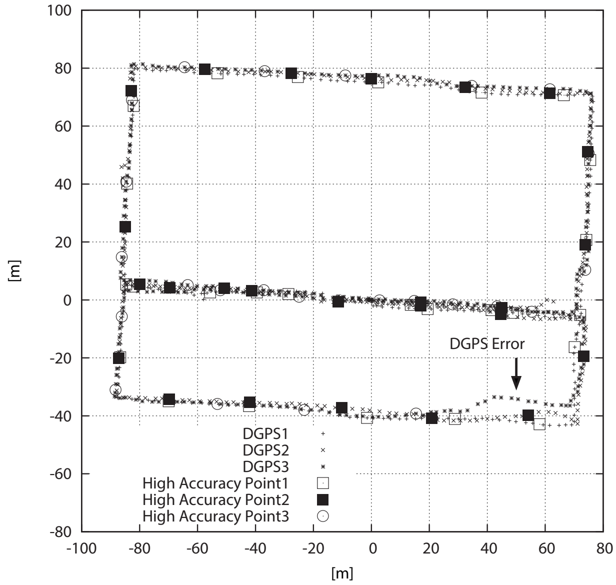

Fig. 4. DGPS trajectories and high-accuracy points.

accordingly, as on the curved roadways. If any curved course were divided into short sections, each of these sections could be regarded as a straight line. Based on the experience gained in the navigation experiments in the Tsukuba Challenge project, we have set the distance of such short sections at 5 m. We have set the number of DGPS positioning points at seven for an approximate line, in view of the facts that (1) the robot's navigation speed has been set at 0.7 m/s, slightly slower than that of an average pedestrian, and (2) the updating cycle for DGPS positioning is 1 Hz. When the contribution rate of the first principal component of an approximate line is 0.999 or more, it is defined as a DGPS high-accuracy point. If any curved roadway or fork where a big change in navigation direction is involved in the line of DGPS positioning points, then the contribution rate of the first principal component will decrease and no high-accuracy points will be extracted.

Figure 4 illustrates the DGPS positioning trajectories and extracted high-accuracy points when the robot was manually pushed to navigate the course three times. DGPS3 in **Fig. 4** has a section (enclosed by a broken line) in which positioning accuracies are particularly low, probably due to multipath caused by the buildings. There are several more low-accuracy sections that are probably caused by multipath. On the other hand, most high-accuracy points are extracted from straight navigation sections where positioning accuracies are relatively high. Our new method, however, finds it difficult to adequately cope with things such as offset positioning errors that come up along buildings. To decrease such errors, therefore, we have used scan matching for loop closing, as described below.

3.3. Estimation of Trajectories

We estimate the robot's trajectories with the framework of a particle filter, where the robot's probabilistic positions and attitudes are represented by particles [13]. In general, a particle filter consists of two steps, prediction and resampling. In prediction step, position and attitude of each particles are predicted using the motion model. In resampling step, likelihoods of particles are calculated using measurement data such as scan matching and DGPS positioning. Particles with high likelihood are resampled. The robot's trajectory corresponds to the trajectory of maximum likelihood particle.

3.3.1. Motion Model

With v_t denoting the robot's speed at time t as obtained by the odometry and M denoting the total number of particles, the motion model of the k-th particle $\left({}^f_k x_{(t)}, {}^f_k y_{(t)}, {}^f_k \theta_t\right)$ is expressed by Eqs. (1), (2), and (3). In Eq. (3), ${}^f_k \phi_t$ is the accumulated error of gyro. ${}_k\sigma_t$ and ${}_k\omega_t$ are random numbers, which represent measurement noises, conform to normal distribution.

We have set the total number of particles M to 100. We use the trajectory of the final most likely particle for the occupancy grid mapping.

$$ {}^f_k x_{(t)} = \int (v_t + {}_k\sigma_t) \cos {}^f_k \theta_t dt \quad \ldots \ldots \quad (1) $$

$$ {}^f_k y_{(t)} = \int (v_t + {}_k\sigma_t) \sin {}^f_k \theta_t dt \quad \ldots \ldots \quad (2) $$

$$ {}^f_k \theta_t = {}^g\theta_t + {}^f_k \phi_t + {}_k\omega_t \quad \ldots \ldots \quad (3) $$

$$ {}_k l_t = \sqrt{\left({}^p x_t - {}^f_k x_{(t)}\right)^2 + \left({}^p y_t - {}^f_k y_{(t)}\right)^2} \quad \ldots \quad (4) $$

$$ {}_k w_t = \frac{1}{\sqrt{2\pi}\sigma_d} \exp\left(\frac{-{}_k l_t^2}{2\sigma_d^2}\right) \quad \ldots \ldots \quad (5) $$

$$ {}_k r_t = \frac{{}_k N_t}{N} \quad \ldots \ldots \quad (6) $$

$$ {}^f_k w_t = \frac{1}{\sqrt{2\pi}\sigma_d} \exp\left(\frac{-\alpha(1 - {}_k r_t)^2}{2\sigma_d^2}\right) \quad \ldots \quad (7) $$

$$ {}^p_k w_t = \cos\left({}^f_k \theta_t - {}^p\theta_t\right), \quad (0 \le k \le M-1) \quad . \quad (8) $$

3.3.2. Localization on DGPS High-Accuracy Points

Localizations using DGPS high-accuracy points are performed in unknown areas through which the robot passes for the first time. Distances between each particle and high-accuracy points are defined as likelihood. The distance between DGPS high-accuracy point $({}^p x_t, {}^p y_t, {}^p \theta_t)$ extracted at time t and the k-th particle is denoted by ${}_k l_t$. As likelihood becomes greater with particles closer to high-accuracy points and the maximum value set at 1.0 or less, likelihood ${}_k w_t$ is expressed by Eq. (5).

Figure 5 illustrates the trajectories given by the gyro-odometry after the robot had navigated the course three times. The wildly distorted shapes of the trajectories seem to have been caused by accumulated errors. Specifically, errors seem to have accumulated at the corners of the course where the direction of navigation changes at nearly a right angle. **Fig. 6** illustrates the trajectories estimated by the particle filter with the odometry and high-accuracy DGPS points. Mismatches in the trajectories are 2 m at the maximum in the overlapped section R1. **Fig. 7** illustrates the occupancy grid maps generated with PF3. These maps present the largest DGPS positioning errors. Unconformity is also recognized in the observations of an identical landmark (exterior wall of the building) in the overlapped section R1. Such unconformity is resolved by loop closing, as explained below.

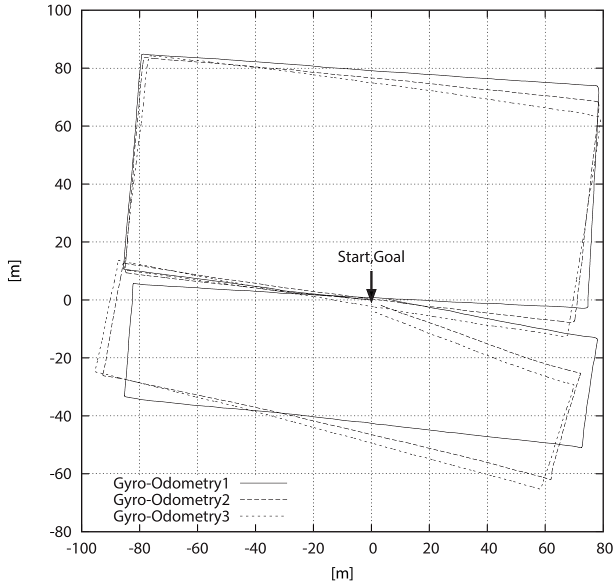

Fig. 5. Trajectories of gyro-odometry.

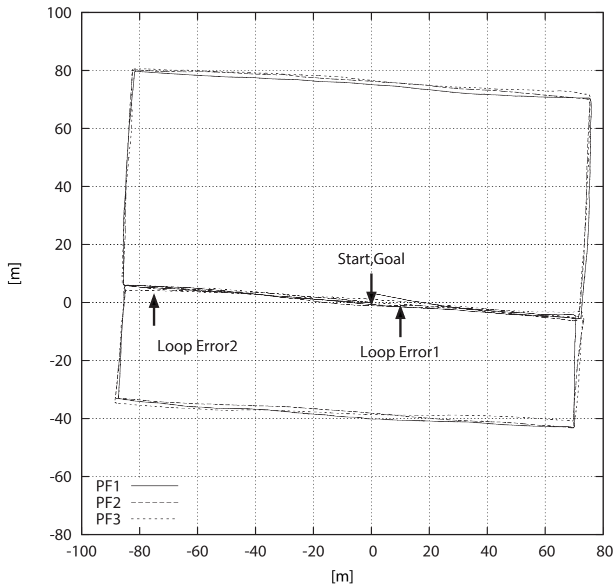

Fig. 6. Estimated trajectories by DGPS high-accuracy points.

3.3.3. Using Scan Matching for Loop Closing

Scan matching is performed in the known areas where the robot has passed more than once. Accuracies in scan matching are evaluated on the matching rates between scan data for each particle and the landmarks on the oc-

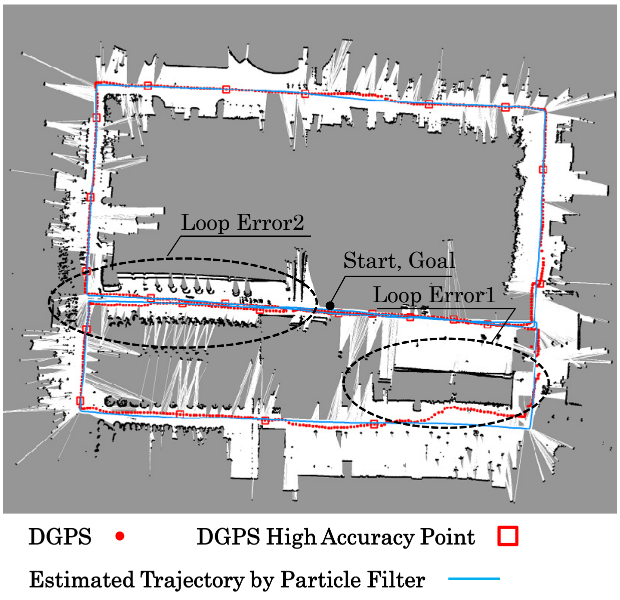

Fig. 7. Occupancy grid map with DGPS high-accuracy points.

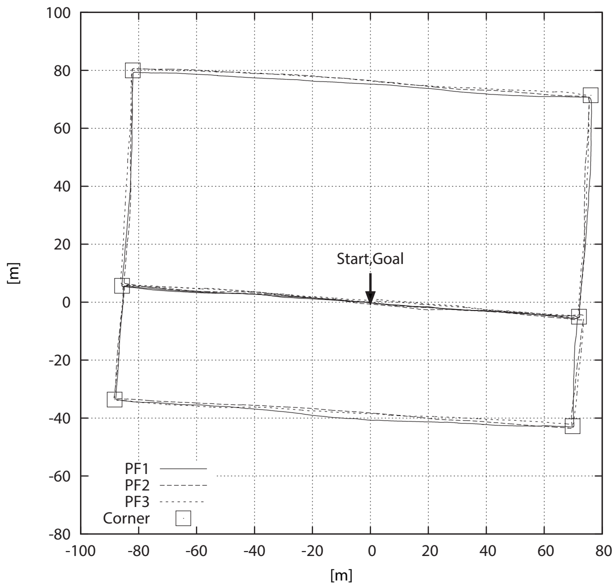

Fig. 8. Trajectories estimated using DGPS high-accuracy points and loop closing method.

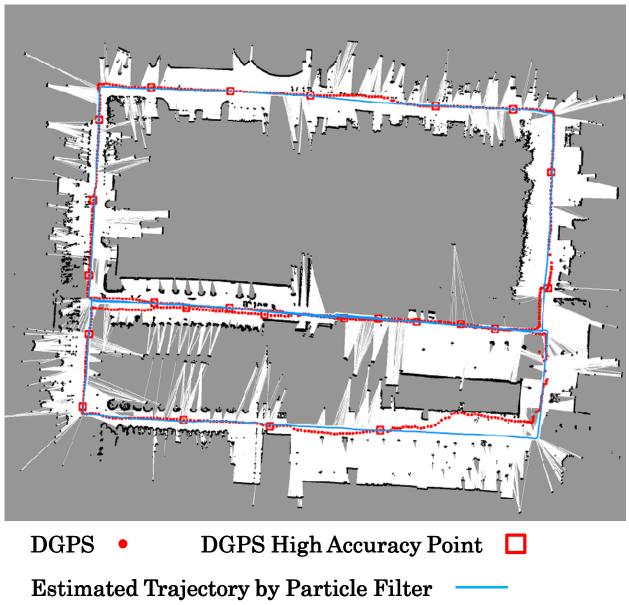

Fig. 9. Occupancy grid map with DGPS high-accuracy points and loop closing method.

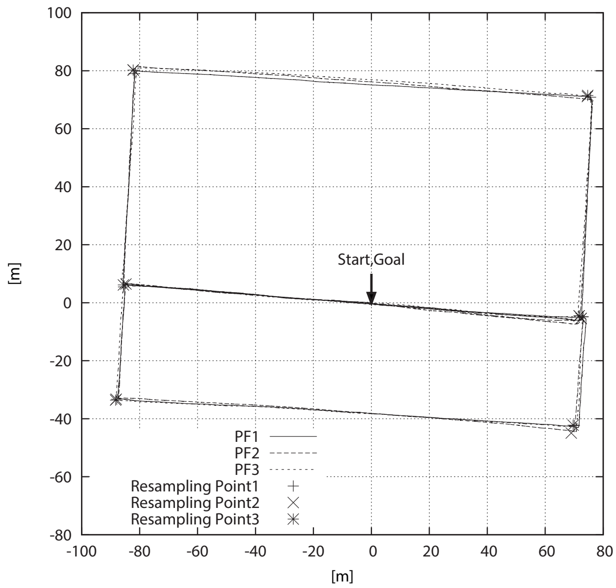

Fig. 10. Trajectories estimated using DGPS high-accuracy points, loop closing method and corners.

cupancy grid map. With ${}_kN_t$ denoting the number of scan data for the k-th particle that have matched with the map at time t, and with N denoting the total number of scan data from the laser scanner, the matching rates ${}_kr_t$ are obtained from Eq. (6). Likelihood ${}^f_k w_t$ for each particle in scan matching is expressed by Eq. (7), using the matching rates.

Figure 8 illustrates the trajectories estimated using DGPS high-accuracy points and loop closing. The trajectories in the overlapped section R1 are almost identical to those estimated with high-accuracy DGPS points only (**Fig. 6**). **Fig. 9** illustrates the occupancy grid mapping with PF3. We can see from **Fig. 9** that unconformity with the landmarks has been resolved, while the mapping is distorted in the straight sections, probably due to the variability of high-accuracy DGPS points.

3.3.4. Higher Accuracies in Estimations of Trajectories at Corners

The trajectories estimated using loop closing in **Fig. 8** present relatively high accuracies around the corners (marked "Corner" in **Fig. 8**). For the sake of generating much higher-accuracy occupancy grid map, we have set resampling points on the corners using loop closing to re-estimate the trajectories in the known areas.

Figure 10 illustrates the trajectories estimated in the abovementioned way. Three trajectories were found to be almost identical to each other all around the course. As compared with the trajectories estimated using DGPS positioning points and loop closing in **Fig. 8**, **Fig. 10** shows far fewer distortions in the straight sections, represent-

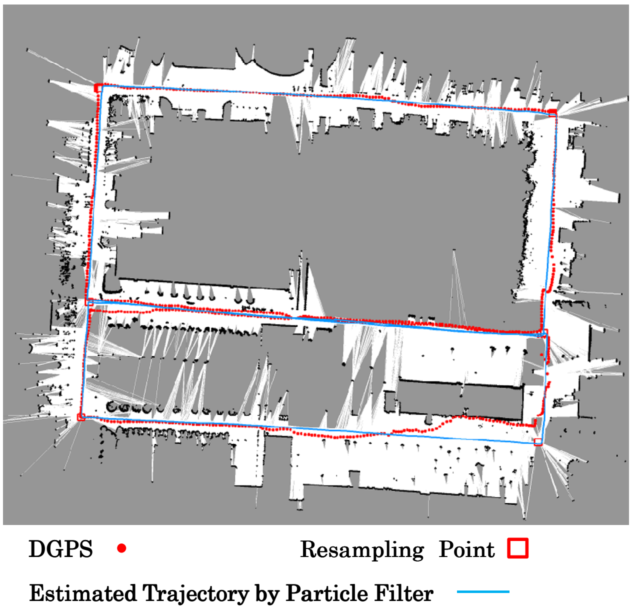

Fig. 11. Occupancy grid map with DGPS high-accuracy points, loop closing method and corners.

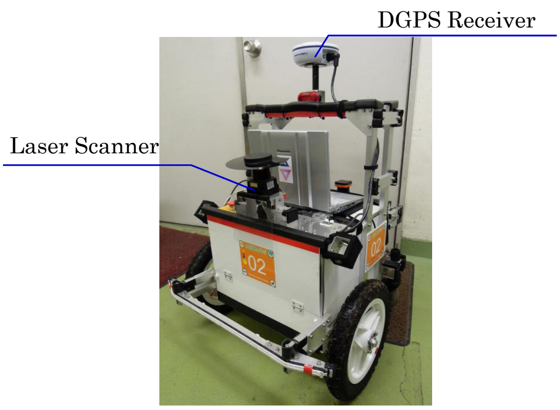

Fig. 12. Robot.

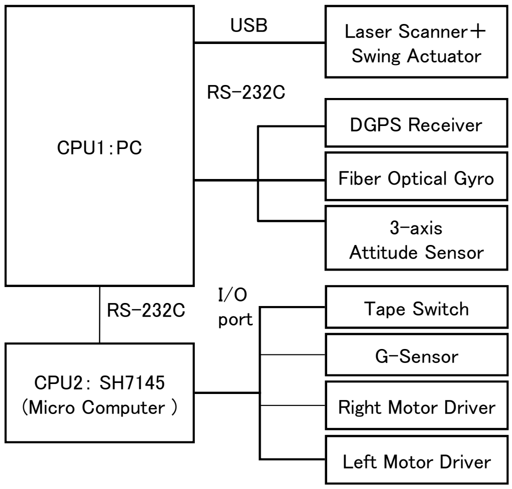

Fig. 13. System configuration.

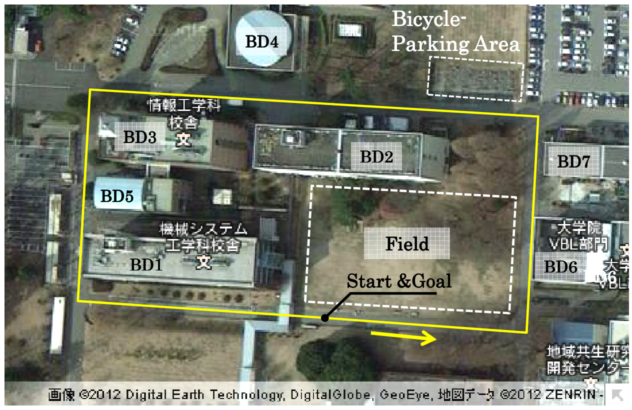

Fig. 14. Course environment.

ing the trajectories with much higher accuracy or reproducibility. **Fig. 11** illustrates the occupancy grid mapping for the trajectory of PF3, which was found to be very accurate in the directions and shapes. We then combined the use of DGPS positioning and scan matching with this map for localizations.

4. Experiments

Through autonomous navigation experiments, we verified the effectiveness of the proposed method of localizations using a combination of DGPS positioning and scan matching.

4.1. Experimental System

For the experimental system, we used the mobile robot shown in **Fig. 12**. The system configuration is illustrated in **Fig. 13**. The robot has encoders fitted in the left and right wheels to calculate the translational distances and attitudes. We used an optical fiber gyro (HOFG-OLC-1; Hitachi Cable, Ltd.) for much more accurate measurements of the robot's attitudes. The DGPS receiver installed in the system was the Hemisphere A100, which only uses GGA sentences in NMEA183 format as positioning data. The updating cycle was set to 1 Hz to secure an adequately-wide distance between the positioning points. The robot had a laser scanner (TopURG; Hokuyo Electric Co., Ltd.) installed at the front for external sensing purposes. The laser scanner could scan the front of the robot over $\pm 135°$ in the range of 30 m in distance to sense the space and shapes of objects.

4.2. Experimental Environment

We set up an experimental course approximately 470 m in length on the campus of the Faculty of Engineering, Utsunomiya University (Japan). **Fig. 14** illustrates the course environment. The course was a circuit with the same point as the starting point and goal. Around it were relatively few buildings that could interfere with DGPS positioning, so ample open air space was left over the robot. There were few landmarks in about the first 50 m,

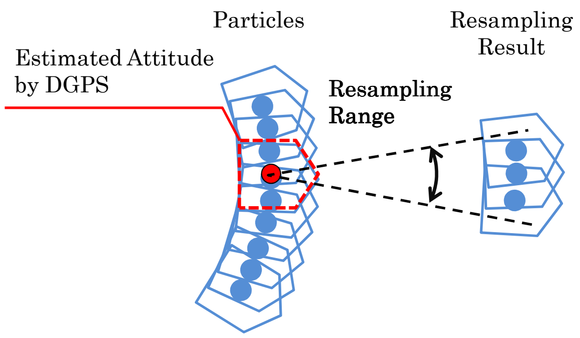

Fig. 15. Resampling using DGPS.

but there were multiple buildings along the course thereafter. DGPS positioning accuracies most likely decreased due to multipath, particularly in the section between BD2, 3 and BD4, each of which were as tall as 40 m. Multipath was also possible around BD1, 5, 6, 7. We estimated the robot's trajectories and created the occupancy grid maps for this course with decreased DGPS positioning accuracies. For the occupancy grid mapping, the robot was manually pushed along the course.

4.3. Resampling Using DGPS Positioning and Scan Matching

Resampling using DGPS positioning was aimed at preventing any mismatching in scan matching. Given some errors involved in the robot's positions estimated by DGPS positioning, it was difficult to make them correspond to the results of scan matching. On the other hand, the robot's attitudes estimated on the lines of DGPS positioning points were found to be relatively high in accuracy, as mentioned previously. Therefore, the robot's attitudes estimated on the line of positioning points were used for resampling by DGPS positioning, as illustrated in **Fig. 15**. Likelihood was calculated with the inclinations ${}^{p}\theta_t$ of the approximate line to the line of DGPS positioning points and the attitudes of particles ${}^{f}_{k}\theta_t$, as expressed by Eq. (8).

The occupancy grid map was found to be almost identical to DGPS positioning in terms of directions. Resampling through DGPS positioning was done only for the attitudes. No unconformity was, therefore, expected to occur between DGPS positioning and scan matching in terms of the robot's positions. In addition, resampling using DGPS positioning makes the particles converge, which serves to prevent mismatching due to the spread of particles in the environments in which scan matching cannot be appropriately applied.

4.4. Experiments of Autonomous Navigation

We verified the effectiveness of the combined use of DGPS positioning and scan matching for localizations through a comparison with localizations through scan matching only. **Fig. 16** illustrates the localizations done by resampling the particles with the likelihood given by

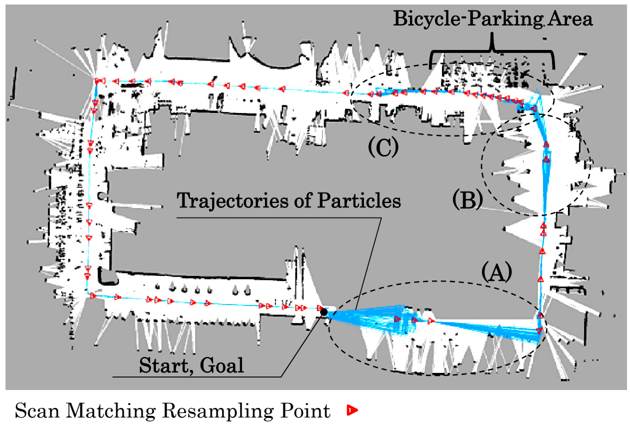

Fig. 16. Trajectories of particles by resampling using scan matching.

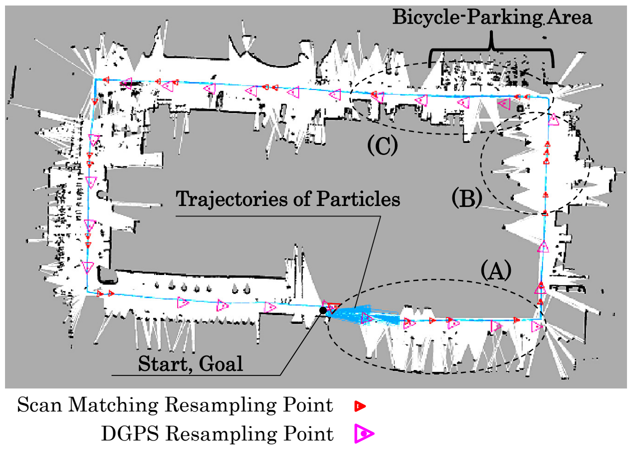

Fig. 17. Trajectories of particles by resampling using scan matching and DGPS.

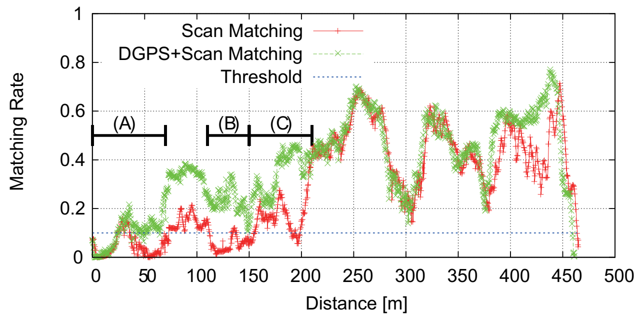

Fig. 18. Evaluation of scan matching.

scan matching only, while **Fig. 17** illustrates the localizations with the likelihood given by both of DGPS positioning and scan matching. The latter figure also shows the resampling points given by DGPS positioning. **Fig. 18** illustrates the matching rates of the maximum likelihood particles or maximum matching rates $Max({}_{k}r_t)$. They are hereinafter called "Matching Rates" only.

Let us now elaborate on the results of localizations done using the two methods. In **Fig. 16**, there are so few landmarks in Section (A) that localizations done using scan matching only show lower matching rates than the threshold values, forgoing the resampling of particles and, as a result, spreading them. On the other hand, **Fig. 17** for the localizations through the combined use of DGPS positioning and scan matching shows that the resampling of particles was done using DGPS positioning five times in the same section with a result of particles spread much less.

As there are a few landmark buildings in Section (B), localizations done using scan matching only in **Fig. 16** show the particles to be better converged, but there are rather large errors in the front-to-back direction of the robot, which seem to be due to the effects of the initial errors in Section (A). The localizations done using a combination of DGPS positioning and scan matching in **Fig. 17** show the particles to be well converged, which suggests very highly accurate localizations in the environments. **Fig. 18** illustrates the evaluations of using scan matching for localization. The localizations done with a combined use of DGPS positioning and scan matching were found to be very accurate and with relatively high matching rates, while those done with scan matching only had some mismatches. This was due to some unconformity in the robot's positions and attitudes, leading to lower matching rates.

Section (C) had a few buildings on the left and a bicycle parking area on the right. As many people entered and exited the parking area, parking their bicycles in any available spots, some mismatching between scan data and landmarks was bound to be observed in the section; such mismatching was most likely on the opposite side of the bicycle parking area, which had no buildings around it. The localizations done using scan matching only would most likely cause positional mismatches and get particles converged in positions distant from actual ones. If such mismatching were to continue on some lengths of the course, the robot would probably deviate from the course. **Fig. 18**, which illustrates the evaluations of scan matching, shows large variability, suggesting failures in localization. On the other hand, the combined use of DGPS positioning and scan matching generated accurate and stable localizations from the beginning to the end of the section. It also gained constantly high evaluations in terms of matching rates.

The sections after Section (C), surrounded by buildings, were perfect environments for scan matching, where stable localizations without mismatching were done using scan matching only, with no use of DGPS positioning. If mismatching were to continue for some lengths, however, the robot could deviate from the course, forcing it to suspend its autonomous navigation. On the other hand, combined use of DGPS positioning and scan matching with generally high matching rates in all the sections of the course demonstrated stable autonomous navigation.

4.5. Reproducibility of Autonomous Navigation

Figure 19 illustrates the robot's trajectories in three-consecutive-successful autonomous navigations through

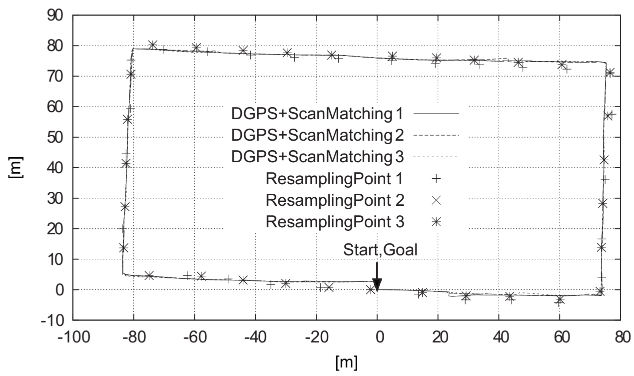

Fig. 19. Trajectories of autonomous navigation.

the combined use of DGPS positioning and scan matching. The maximum error in the trajectories throughout the course was about 1 m. The fact that resampling of the particles by the line of DGPS positioning points was done at nearly the same spots seems to prove the reproducibility of the positional estimations by the line of DGPS positioning points as well as its adequate resampling accuracies.

5. Consideration

In this study, we used DGPS positioning to create occupancy grid maps in order to make up for the shortcomings of scan matching. We conducted autonomous navigation experiments to verify how much such shortcomings of scan matching were corrected. We now elaborate on the shortcomings of scan matching.

Scan matching is likely to fail, for example, at intersections with few landmarks where the robot must change course as shown in **Fig. 16**. In this study, mismatching occurred in the section of the course with a bicycle parking area and few buildings. This seems to have been caused by the following two things:

- The particles were spread in the section with few landmarks up to the point where the course changed.
- The robot underwent significant attitude changes at the turning points of the course, and these altered the directions from which landmarks were observed. This made the shapes appear different from the ones previously observed.

Compared with the localizations done using scan matching only, those done through the combined use of DGPS positioning and scan matching proved more advantageous in terms of the following. As the spread of the particles is found to be preventable by using resampling based on localizations done using DGPS positioning, we can concentrate them in the positions where a high degree of conformity with scan matching can be expected. This in turn serves to achieve relatively high matching rates or stable localizations.

6. Conclusions

Described in this paper is our proposal for occupancy grid mapping with loop closing through the combined use of DGPS positioning and scan matching. We have conducted experiments to demonstrate the localizations of an autonomously navigating robot using the combination of DGPS and scan matching. We have used the framework of a particle filter for the combination of DGPS positioning and scan matching. We have confirmed that the particle spread can be prevented by resampling them on the attitudes estimated from the line of DGPS positioning points, which in turn has made up for any shortcomings in scan matching. Stable autonomous navigation has thus been achieved.

References:

[1] S. Yuta, M. Mizukawa, and H. Hashimoto, "Tsukuba Challenge: The Purpose and Results," J. of the Society of Instrument and Control Engineers, Vol.49, No.9, pp. 572-578, 2010 (in Japanese).

[2] K. Irie, T. Yoshida, E. Koyanagi, and M. Tomono, "A Localization Method Using Gyro-assisted Odometry and 3D Laser Scanner Considering Gyro Drift Error," 2010 JSME Conf. on Robotics and Mechatronics, 1A1-E01, 2010 (in Japanese).

[3] M. Yokozuka, Y. Suzuki, T. Takei, N. Hashimoto, and O. Matsumoto, "Auxiliary Particle Filter Localization for Intelligent Wheelchair Systems in Urban Environments," J. of Robotics and Mechatronics, Vol.22, No.6, pp. 758-765, 2010.

[4] T. Tomizawa, S. Muramatsu, M. Sato, M. Hirai, S. Kudoh, and T. Suehiro, "Development of an Intelligent Senior-Car in a Pedestrian Walkway," Advanced Robotics, Vol.26, No.14, 2012.

[5] H. Date and Y. Takita, "Real world experiments of an autonomous mobile robot in the pedestrian environment," in: Proc. 5th Int. Conf. on Automation, Robotics and Applications, pp. 413-418, Wellington, New Zealand, 2011.

[6] T. Suzuki et al., "The Possibility of the Precise Positioning and Multipath Error Mitigation in the Real-time," The 2004 Int. Symposium on GNSS/GPS, 2004.

[7] K. Ohno, T. Tsubouchi, B. Shigematsu, and S. Yuta, "Differential GPS and odometry-based outdoor navigation of a mobile robot," Advanced Robotics, Vol.18, No.6, pp. 611-635, 2004.

[8] E. Takeuchi, M. Yamazaki, K. Ohno, and S. Tadokoro, "GPS Measurement Model with Satellite Visibility using 3D Map for Particle Filter," 2011 IEEE Int. Conf. on Robotics and Biomimetics (ROBIO 2011), 2011.

[9] M. Kitamura, T. Suzuki, Y. Amano, and T. Hashizume, "Improvement of GPS and GLONASS Positioning Accuracy by Multipath Mitigation Using Omnidirectional Infrared Camera," J. of Robotics and Mechatronics, Vol.23, No.6 pp. 1125-1131, 2011.

[10] Y. Hara, H. Kawata, A. Ohya, and S.Yuta, "Map Building for Mobile Robots using a SOKUIKI Sensor – Robust Scan Matching using Laser Reflectance Intensity –," SICE-ICASE Int. Joint Conf. 2006, SE14-4, 2006.

[11] H. Date and Y. Takita, "Real World Experiments of Autonomous Mobile Robot Smart Dump – Influence and Countermeasure of Human Crowd Behavior in a Pedestrian Environment –," J. of Robotics Society of Japan, Vol.30, No.3, pp. 305-313, 2012 (in Japanese).

[12] Y. Morales, E. Takeuchi, and T. Tsubouchi, "Vehicle Localization in Outdoor Woodland Environment with sensor fault detection," Proc. of the ICRA 2008, pp. 449-454, 2008.

[13] M. Montemerlo, S. Thun, D. Koller, and B. Wegbreit, "FastSLAM: A factored solution to simultaneous mapping and localization," in: Proc. National Conf. on Artificial Intelligence (AAAI), 2002.

Name:
Junji Eguchi

Affiliation:
Doctor Student, Department of Innovation Systems Engineering, Utsunomiya University

Address:
7-1-2 Yoto, Utsunomiya-city, Tochigi 321-8585, Japan

Brief Biographical History:
2000- Joined Automobile R&D Center, Honda R&D Co., Ltd.

Main Works:
• "Development of Navigation Method for Autonomous Mobile Robot based on Waypoints Tracking Set by using of DGPS," J. of Robotics Society of Japan, Vol.30, No.3, pp. 314-323, 2012.

Membership in Academic Societies:
• Society of Automotive Engineers of Japan
• The Japan Society of Mechanical Engineering (JSME)
• The Robotics Society of Japan (RSJ)

Name:
Koichi Ozaki

Affiliation:
Graduate School of Utsunomiya University

Address:
7-1-2 Yoto, Utsunomiya-city, Tochigi 321-8585, Japan

Brief Biographical History:
• 1996-2003 Assistant Professor, Utsunomiya University
• 2003-2010 Associate Professor, Graduate School of Utsunomiya University
• 2011- Professor, Graduate School of Utsunomiya University

Main Works:
• "Application of Localization Based on DC Magnetic Field Occurred in the Environment on Wheel Type Mobile Agricultural Robots," The Int. J. of the Robotics Society of Japan, Advanced Robotics, Vol.25, No.5, pp. 923-939, April 2011.

Membership in Academic Societies:
• The Japan Society of Mechanical Engineering (JSME)
• The Robotics Society of Japan (RSJ)
• The Japan Society of Kansei Engineering (JSKE)